Indian Journal of Pure & Applied Physics
Vol. 63, April 2025, pp. 301-311
DOI: 10.56042/ijpap.v63i4.14412

# A Novel Planar Antenna with Mushroom Shaped DGS for WBAN Applications

Lily Kumari[a,b*], Munna Khan[a] & Zahreeuddin[a]

[a] Department of Electrical Engineering, FET Jamia Millia Islamia, New Delhi 110 025, India

[b] Electronics and Communication Engineering, Dronacharya Group of Institutions, Greater Noida 201 306, India

*Received: 15 October 2024; accepted: 1 April 2025*

In this paper, a compact, low profile planar antenna has been proposed with a mushroom shaped defective ground structure at the back, for WBAN and biomedical applications. This proposed antenna is designed and fabricated on a semi flexible board of RT/duroid 5880 substrate with dimensions 66 × 66 × 1.64 $mm^3$. The proposed QCCR (Quad Corner Cut Ring) antenna is combination of patch and defective ground structure, exhibit impressive impedance bandwidth of 500 MHz (bandwidth percentage 8.7%), spanning from 5.5 to 6 GHz and also shows a substantial gain of 7.25 dBi in free space. The designed antenna resonates at frequency 5.68 GHz and 5.92 GHz for return loss better than -10dB and provides good impedance matching even when placed on body phantom. To achieve the impedance bandwidth within Spectrum range of Wireless Body Area Network (WBAN), DGS technique was implemented. The radiation efficiency is 98.72% for the designed antenna. Furthermore, the incorporation of the defective ground structure has a significant positive impact on bandwidth enhancement of antenna. A comprehensive simulation analysis and parameter measurement is carried out for different cases, when the antenna is placed in free space, against the body phantom and on bending structure condition. Both simulations and experimental tests confirm the robustness of this defective ground antenna's performance against structural alterations such as bending. The parametric analysis of antenna has been done to achieve the best performance of antenna in all the cases. The purposed antenna SAR value is within range which satisfies the IEEE and FCC standard safety guidelines. The outcomes of these investigations position the proposed planar antenna as a highly promising option for wireless biomedical devices, showcasing its potential to revolutionize the biomedical field applications.

**Keywords:** Planar antenna, Industrial scientific and medical**(**ISM)band, SAR (Specific absorption rate), Biomedical antenna, WBAN(Wireless body area network), Human body phantom, Defective ground structures(DGS), Body area network(BAN), CST-MWS, Quad corner cut ring (QCCR)

## 1 Introduction

In recent years, biomedical telemetry systems have become vital in diverse applications, including health monitoring through wearable bands, emergency or warfare survivor rescue operations and wireless transmission of bio-signals of patients. Biomedical antennas play a pivotal role in these systems, facilitating the transmission of bio-signals between sensors and biomedical devices for both off-body and on-body applications[1,2]. The important consideration for designing of biomedical antenna is light weight, compact, low profile, easy fabrication, flexible and integration with biomedical telemetry systems. Along with these, SAR analysis and bending analysis are the crucial points for the designing of BAN antenna. These antennas, operate in close proximity to the human body, undergo a thoughtful design process. The lossy nature of the human tissue, result in degradation of radiation and operating frequency detuning, its impact is analyzed by the critical parameter electromagnetic coupling. Another, significant consideration involves the absorption of electromagnetic radiation by the human body when an antenna is used for health monitoring. This absorption may pose health risks associated with long-term irradiation[3,4]. Therefore, adhering to health and safety standards, BAN antennas should be designed to emit minimal power absorbed per unit mass, as quantified by the specific absorption rate (SAR). When the BAN antennas are worn on human body, they should possess flexibility, a low profile, and the ability to conform well to the contours of the human body. Regulatory agencies, such as Federal Communications Commission (FCC), have designated specific frequency bands for these biomedical applications, ensuring international acceptability and compliance with standardized frequencies worldwide. The frequency range designated for Medical Body Area Networks (MBANs) is 2.4 GHz to 2.48 GHz, while for WBANs, it spans from 5.75 GHz to 5.85 GHz[5,6]. These

*Corresponding author: (E-mail: lilygupta14dec@gmail.com)

allocated frequency bands facilitate the development and deployment of biomedical planar antennas, ensuring compatibility and standardized communication within the specified ranges for MBAN and WBAN. Biomedical planar antennas are typically designed for applications such as Medical Body Area Network (MBAN), WBAN, and implantable devices. Microstrip patch antennas are commonly employed in biomedical applications due to their compact design, simplicity in fabrication, seamless integration and cost-effectiveness. However, a notable drawback of these planar antennas is their limited bandwidth[7]. To address the issue of low bandwidth in planar antennas, multiple techniques have been identified for enhancing their operating bandwidth and gain. Despite this limitation, microstrip patch antennas offer a significant advantage in terms of their compact nature[8,9]. In recent years, several techniques such as Frequency Selective Surface (FSS), Electromagnetic Band Gap (EBG), Photonic Band Gap (PBG) and metamaterial has implemented for parameter (bandwidth) enhancement[10-12]. In this paper, antenna design incorporates a Defective Ground Structure (DGS) positioned at the back of the patch. The DGS technique, incorporates defects and the slots in the ground of patch antenna designs. Here, mushroom shaped DGS structure is etched at the ground plane. It is the modified and the easy form of the EBG structure. The implementation of DGS structure make to antenna design more compact and easier to fabricate than the EBG and PBG. The inclusion of DGS in the design offers a distinct advantage in enhancing the bandwidth of the proposed antenna. For instance, reference[13] presents a fractal antenna designed for a frequency of 2.4 GHz in the ISM band. The significant drawback of this design lies in the impedance mismatch caused by the loading effect of the human body. Another example is a triangular patch antenna that was developed, encountering limitations due to its narrow bandwidth[14]. Additionally, a compact slot antenna was created using the CPW feeding technique, resonating at 5.825 GHz within the ISM band. Nevertheless, it possesses a low fractional bandwidth (6% at the resonating frequency)[15]. Several other biomedical antennas have been devised employing techniques like SIW and EBG, but they exhibit low bandwidth and are not very compact[16,17]. Furthermore, a fabric-based wearable biomedical antenna with a copper-based patch was introduced, although its dimensions were large, rendering it unsuitable for integration into biomedical devices[18]. The broadband monopole is used as the main radiator of the antenna, and the gradient feeder structure and etched slot on the ground are used to adjust the matching effect of the antenna port. Implanted antenna design using DGS technique was resonating at operating frequency of 2.5 with gain 3.5dBi was presented in reference[19].An integrated rectangular microstrip patch antenna with DGS has been investigated to enhance polarization purity in the radiated fields[20]. The other advantages of the DGS technique is improvement in gain (dBi), higher mode harmonic suppression and mutual coupling between elements[20-22].However, some of biomedical antennas have been designed and developed to cater to diverse biomedical applications, employing various techniques as follows. A planar EBG-based antenna operating at 2.45 GHz was proposed, achieving a gain of 6.93 dBi. However, the antenna exhibited relatively large dimensions[23].A UWB biomedical antenna with gain 2.8 dBi and 4.8 dBi using CB-CPW technique was discussed[24]. Here, the proposed planar antenna has been designed using the mushroom shaped DGS structure.

## 2 Antenna Design

This paper presents, the configuration of compact intended planar antenna with mushroom shaped defective ground structure. The evolution of the proposed antenna from the conventional rectangular

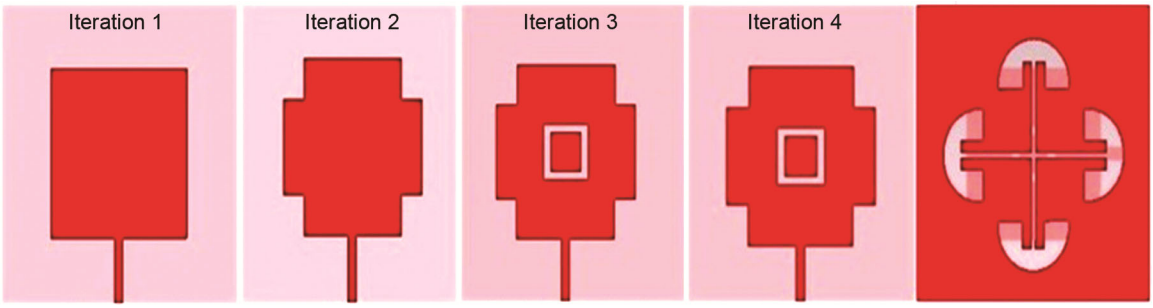


Fig. 1 — Evolution process of patch structure of designed antenna for biomedical applications(Iteration 1 to iteration 4)

design is shown in Fig. 1. It includes four iterations. In Iteration 1, a conventional rectangular patch structure is formulated. Iteration 2 introduces equal corner-cut slots into the rectangular patch. In Iteration 3, a central ring is incorporated into the previous design to enhance performance. Finally, Iteration 4 integrates a DGS (Defected Ground Structure) design into the ground to further improve efficiency. The top view of designed antenna and mushroom shaped defective ground structure with dimensions are shown in Fig. 2(a) & Fig. 2 (b), respectively. The intended antenna consists of a semi-flexible substrate layer (66mm×66mm×1.57mm) of RT/duroid 5880 (with a dielectric constant of 2.2 and a loss tangent of 0.0004 placed on ground layer (66mm×66mm×0.035mm). The proposed antenna parametric, SAR and bending analysis were conducted using CST Microwave Studio with the suitable in-built boundary conditions. In this antenna design, a rectangular patch structure at the top, a substrate layer is in middle and defective ground structure at the bottom. The antenna employs a patch of dimension 18.5mm×18.5mm has corners cut out and a ring structure at the centre creating QCCR. A defective ground is established by connecting mushroom structures with solid lines. In this design a rectangular patch is cut at corner with equal size rectangular (8.5mm×5.5mm).The square ring has an outer square measuring 12mm×12mm and an inner square measuring 8mm×8mm. Figure 3 depicts the simulation setup, where the designed patch antenna is positioned on top of the HUGO human body phantom model measuring 100×100 mm². This model consists of three layers representing human skin, fat, and muscle with dielectric values sourced from the IT'IS Foundation and detailed in Table 1. The designed antenna is place at a distance of 2 mm above the body phantom model to minimize the backward radiation of the antenna. The designed

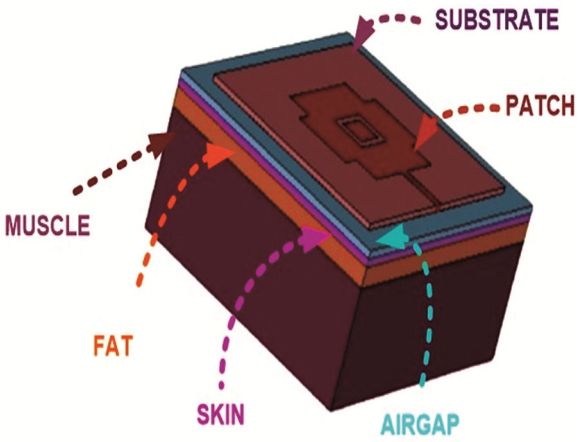


Fig. 3 — DGS technique based proposed antenna is placed on HUGO body phantom model

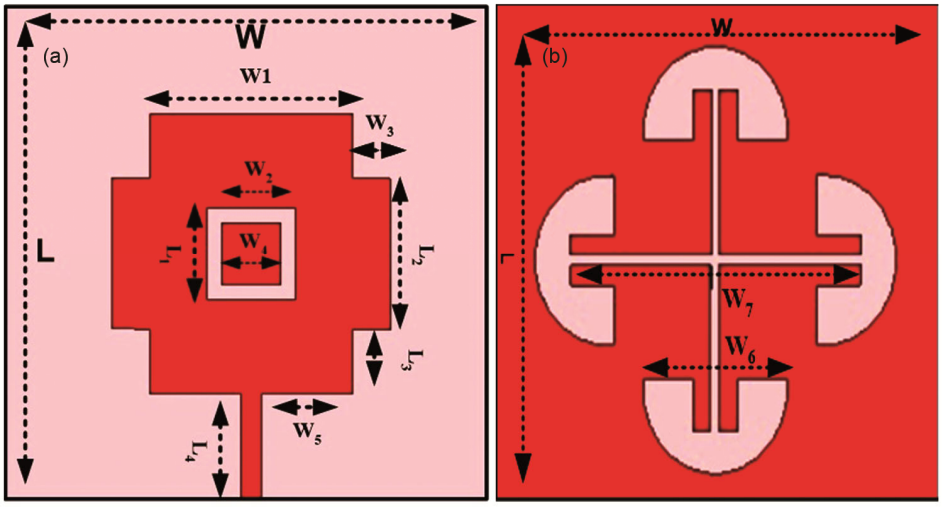


Fig. 2(a) — Top view of the intended antenna, and (b) DGS of antenna [dimensions are in mm, L=66, $L_1$ =12, $L_2$ =20, $L_3$ =8.5, $L_4$ =14.5, W =66, $W_1$ =27, $W_2$ =12, $W_3$ =5, $W_4$ =8, $W_5$ =12.10, $W_6$=19.9, $W_7$=40]

Table 1 — Dimensions of the Human Body Phantom

| Name of human body Phantom model layers | Layer Relative Permittivity ($\varepsilon_r$) | Layer Density (Kg/m$^3$) | Electric Conductivity (S/m) | Thickness (mm) of each layer |
|---|---|---|---|---|
| Skin | 38.1 | 1001 | 1.43 | 2 |
| Fat | 10.8 | 900 | 0.26 | 4 |
| Muscle | 52.8 | 1006 | 1.74 | 28 |

antenna performance has been evaluated by comparing it with the previous published research work[24-31] (Table 2) in context of gain, dimensions and SAR value. The surface current density $J_{surf}$ of the proposed antenna in the free space and with the body phantom are shown in Fig. 4(a-b).

### 2.1 Evolution of Antenna Patch Structure

Evolution process of proposed antenna includes four iteration steps, depicted in Fig. 1 In first iteration, a rectangular patch with plane ground is considered, however the reflection coefficient ($|S_{11}|$) does not lie in the desired frequency range (resonating at 5.66 GHz) and suffers from narrow bandwidth problem and not lie in desired frequency range(bandwidth range 5.62 GHz-5.69 GHz) (Fig. 5). During the second iteration a rectangular slot is cut at all the corners and ground is still a plane structure at the back. However, it is observed that the antenna resonating frequency deviates towards the lower frequency range (4.64 GHz). In third iteration a ring is etched out at the centre of the intended patch design with plane ground structure at the bottom. The after effect of this, the antenna has started operating in two bands (dual band). The analysis revealed that proposed antenna is operating dual band (4.53GHz and 6.89GHz), but not operating with in desired ISM biomedical frequency band. Then in fourth iteration, a defective ground structure is etched out in antenna design. The reflection coefficient ($|S_{11}|$) of iteration 4 antenna structure lies within the ISM frequency range with a gain of 7.25 dBi in free space (Fig. 5). Radiation efficiency and gain are critical parameters in antenna

Table 2 — Comparison of previous work with proposed work

| Ref. | SAR(W/Kg) | Gain (dBi) | Antenna Size($mm^3$) |
|---|---|---|---|
| [24] | 0.24 | 6.93 | 22166 |
| [25] | 0.244 | 5.8 | 17054 |
| [26] | - | 5 | 129870 |
| [27] | 4 | 4.5 | 48223 |
| [28] | <1.6 | 6.12 | 24969 |
| [29] | 0.24 | 6.93 | 12726.3 |
| [30] | <1.6 | 6.55 | 8640 |
| [31] | 0.64 | 6.02 | 22500 |
| Proposed | 0.9 | 7.25 | 7144 |

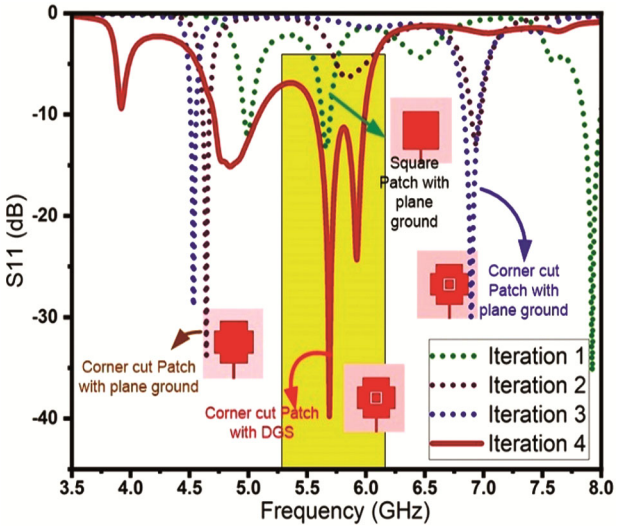


Fig. 5 — Reflection coefficients($|S_{11}|$) analysis of designed antenna during evolution process of patch structure (Iteration 1-4)

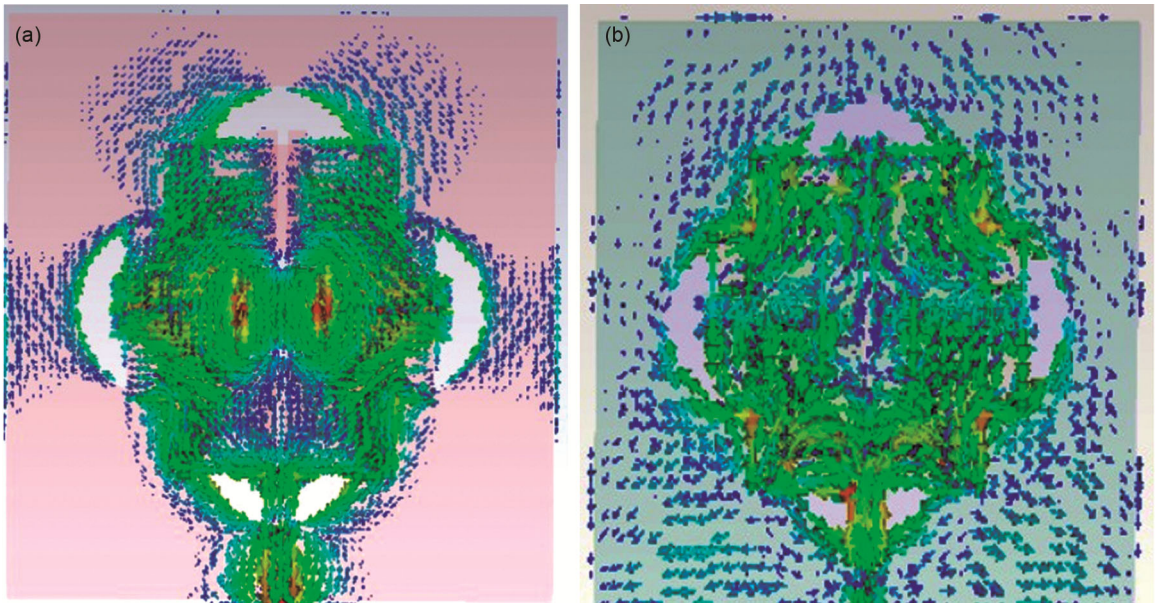


Fig. 4 — (a) Surface current density ($J_{surf}$) of proposed antenna in free space, and (b) Surface current density ($J_{surf}$) of proposed antenna with human body model

design, and their behavior must be carefully analyzed to ensure optimal performance.

The radiation efficiency and gain of all the antenna evolution iterations are simulated and depicted in Figs 6 & 7. It is analyzed that there is improvement of gain 1.05dBi in iteration 4 and 0.19dBi in iteration 3 compare to iteration1 (Fig. 7). The contribution of DGS technique in antenna gain is proximately 1.05dBi. It observed that the improvement in radiation efficiency 11% (Fig. 6) than the iteration design 3 (without DGS structure at bottom).

These characteristic curves allow the designers to achieve optimal results in terms of reflection coefficient, gain and radiation efficiency.

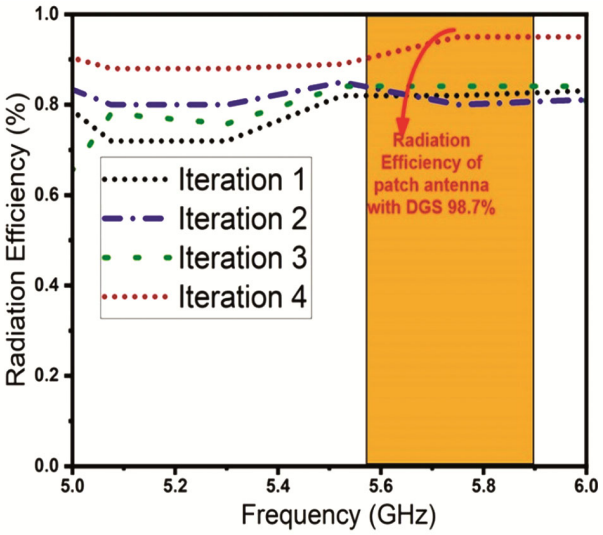


Fig. 6 — Radiation efficiency of designed antenna evolution Process(Iteration1-4)

**2.2 Effect of Defective Ground Structure (DGS)**

In this antenna design, two key aspects are considered in parallel, the top antenna structure and the bottom DGS. This section illustrates the evolution of DGS based ground structure.The antenna design process commenced with the implementation of a plane ground structure. Subsequently, a series of steps were undertaken to achieve the desired mushroom-shaped Defected Ground Structure (DGS).The evolutionary stages of the DGS structure has been depicted in the Fig. 8. The effects of each step were systematically analyzed in terms of reflection coefficients (Fig. 9) and gain (Fig. 10). In the initial stage (Step 1) of the antenna

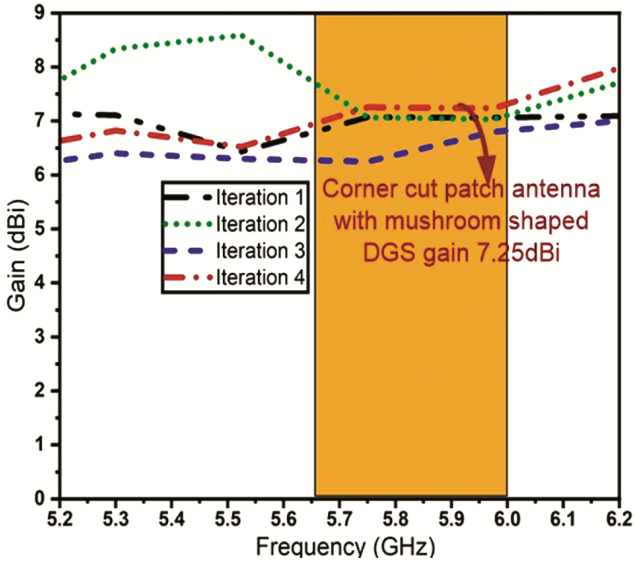


Fig. 7 — Gain (dBi) analysis of designed antenna evolution process (Iteration 1-4)

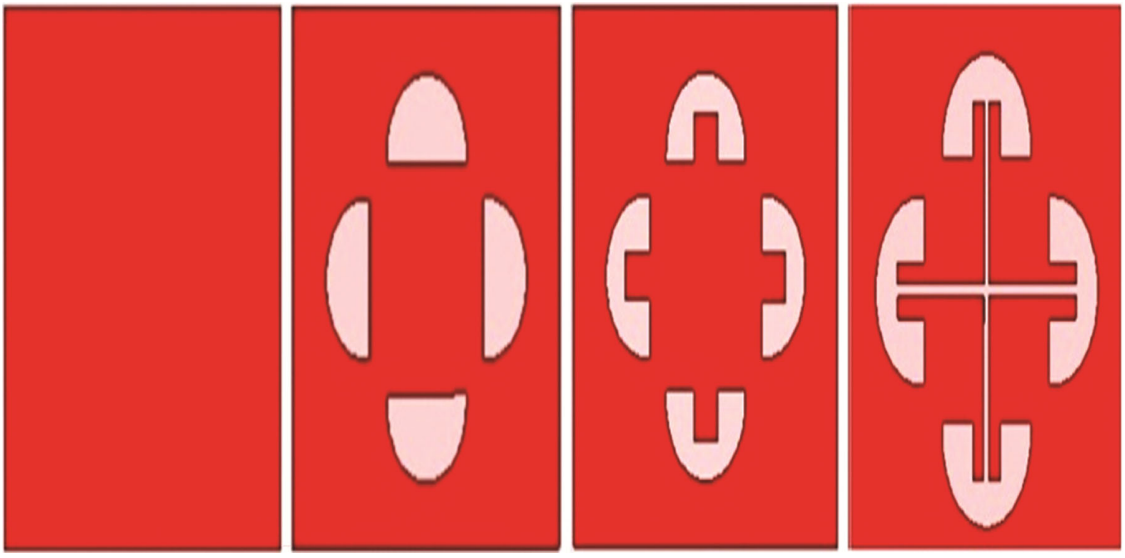

Fig. 8 — Evolution steps of defective ground structure of proposed antenna

design process, the antenna was configured with a flat or plane ground structure.

In step 2, the ground plane underwent a modification wherein four semicircular structures were etched out. In Step 3, further refinement occurred with the addition of four rectangular slots within each semicircle. Finally, in the last step, two lines perpendicular to each other were etched, connecting opposite sides of the rectangular slots within the semicircles. In step 1, the proposed antenna operates in dual bands at frequencies 4.5 GHz and 6.89 GHz, which do not fall within the ISM biomedical frequency range. To address this, semicircle structures have been introduced, resulting in a shift in the lower frequency range from 6.89 GHz to 6.09 GHz. This modification led to a 1 dBi gain improvement than the previous step 1. Following Step 3, a further frequency shift was observed (4.03 GHz and 5.7 GHz), but, these frequencies did not align with the desired frequency range. Moving on to Step 4, both resonating frequencies are combined, resulting in bandwidth extension (150 MHz) and a gain of 7.25 dBi.

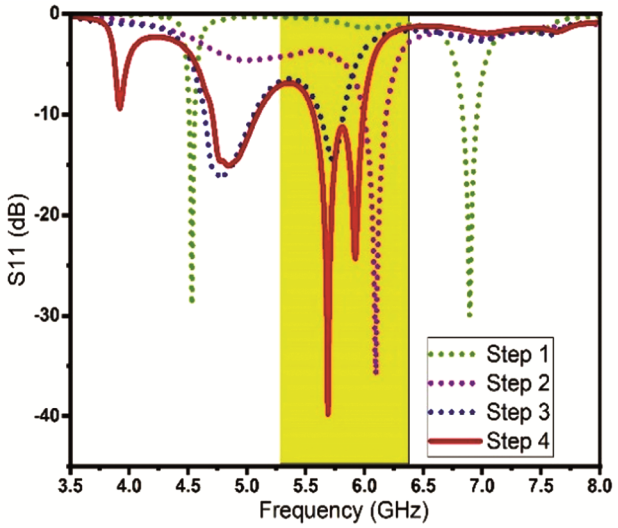


Fig. 9 — Reflection Coefficient analysis of designed antenna evolution Process (step 1-4)

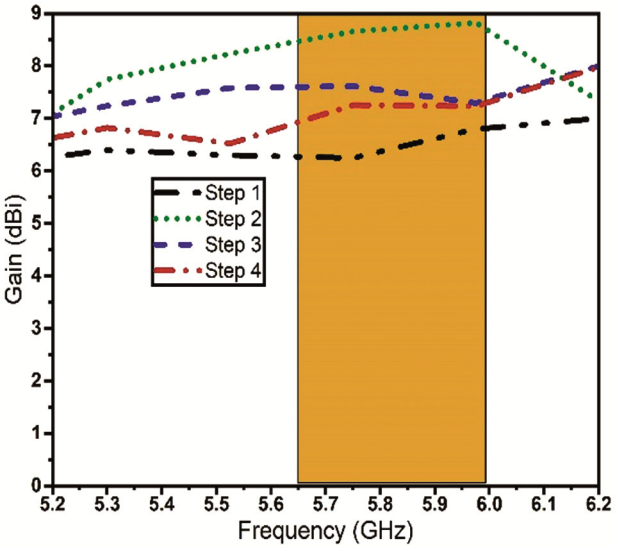


Fig. 10 — Simulated Gain (dBi) analysis of designed antenna during ground evolution steps (1-4)

### 2.3 SAR Analysis

When designing antennas for biomedical applications, two critical parameters are analyzed: SAR and bending analysis. Basically, it is a measure of the rate at which energy is absorbed by the human body when exposed to radiofrequency (RF) electromagnetic fields. SAR is typically expressed in watts per kilogram (W/kg). When antenna is positioned on human body phantom, SAR is given by Eq. (1):

$$SAR = (\rho \times \sigma)/E^2 \quad \ldots(1)$$

where σ is the tissue conductivity in Siemens per meter (S/m), E is the electric field strength in volts per meter (V/m) and ρ is the tissue density in kilograms per cubic meter (kg/m³). It also depends on various other factors, including the frequency of the electromagnetic field and the specific absorption characteristics of different tissues. According to FCC and IEEE guideline the maximum allowable SAR value should be less than 1.6 watts per kilogram (W/kg) averaged over 1 gram of tissue.

### 2.4 Bending Analysis

The designed antenna underwent a parametric analysis, particularly to focus on its performance when subjected to cylindrical surface mimicking the human body arm. The bending analysis involved placing the antenna on cylinders with varying radii (Cr) of 70mm, 80mm, 90mm, and 100mm. Figure 11(a-b) illustrate the bent configuration of the antenna and the corresponding return loss analysis respectively. The results indicate that the antenna exhibits sustained return loss ($|S_{11}|$) within the specified frequency range during the bending process. Consequently, it can be inferred that the antenna parameters remain unaffected by the bending, affirming its suitability for wearable biomedical applications.

## 3 Parametric Analysis

A parametric analysis has been conducted on the intended antenna to optimize its performance by

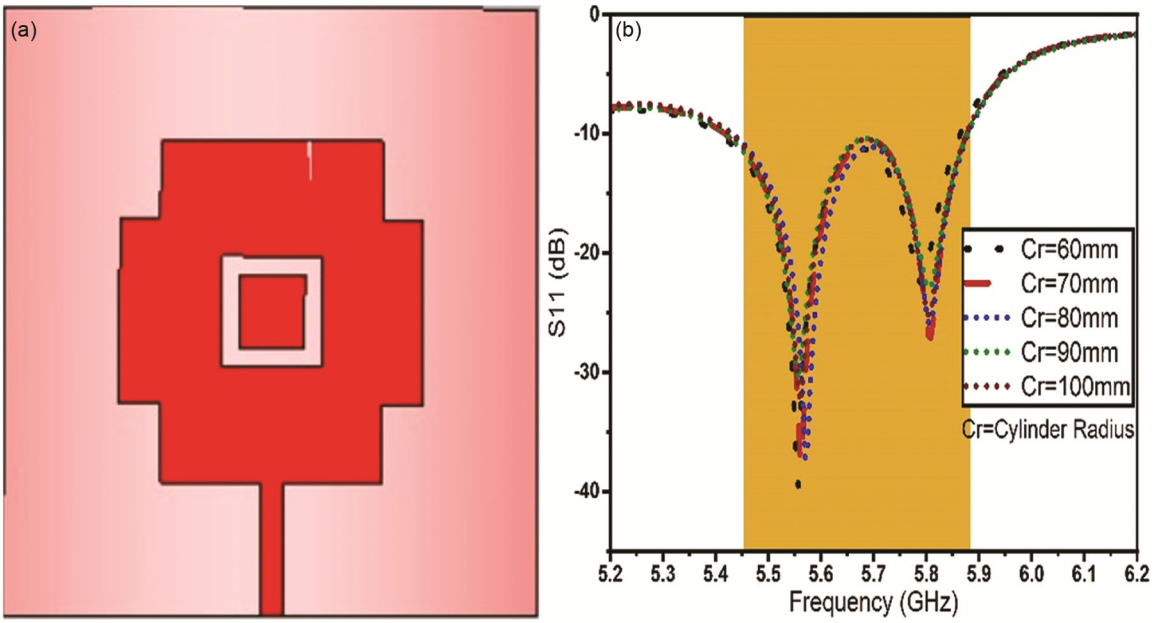


Fig. 11 — (a) Designed antenna is placed on cylinder of different radius for bending analysis, and (b) Reflection coefficients ($|S_{11}|$) analysis, when intended antenna is placed on different cylinder radii($C_r$)

studying various antenna parameters. Here, parametric analysis is implemented on the width of the feedline ($F_w$), position of central the ring and corner cutslot to study parameters such as reflection coefficients ($|S_{11}|$), gain (dBi), radiation efficiency and input resistance ($R_i$). It is observed that the input resistance crosses the 50 Ω line within the WBAN spectrum at $W_4$ = 14.5 mm. In the optimization process of feed line width, the feedline width ($F_w$) is varied to optimize the bandwidth and return loss ($|S_{11}|$) of the designed QCCR antenna within the ISM frequency spectrum shown in Fig. 12. Iinitially, when $F_w$ is set to 1.6 mm, the return loss ($|S_{11}|$) is below -10dB, but the antenna radiates at 4.8 GHz instead of the intended ISM band. Subsequently, adjusting $F_w$ to 2 mm results in a limited bandwidth of the designed antenna, covering a narrow range of 5.7-5.79 GHz, falling short of the desired WBAN. frequency range. Continuing the optimization, setting $F_w$ = 2.4 mm improves reflection coefficient ($|S_{11}|$), but the resonating frequency deviates from the required ISM band. Finally, with $F_w$ at 2.8 mm, the antenna exhibits a promising bandwidth of 5.73 to 6 GHz and achieves a favorable reflection coefficient ( $|S_{11}|$ ) agreement at 5.7 GHz with a value of -39dB, which is within the desired WBAN frequency range. In the quest for antenna optimization, the focus shifted to the parametric analysis of the central ring position (Sr), as depicted in Fig. 13. The square ring has a width of

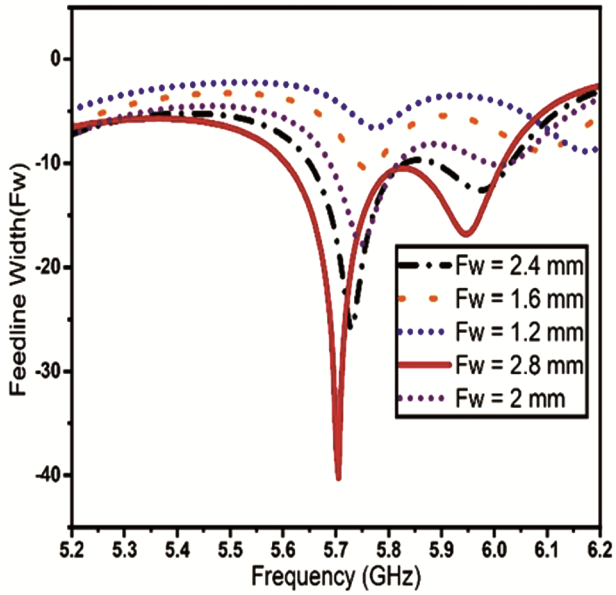


Fig. 12 — Parametric analysis of antenna reflection coefficients ($|S_{11}|$) for various feedline width

4 mm and is positioned at 8mm from the center along both the horizontal and vertical axes. The analysis is done by placing the ring of 4mm at different position. The exploration began by relocating the ring to Sr = (15×11)mm. However, the antenna, which had been carefully designed for the desired operating frequency range, experienced a deviation towards lower frequencies. At Sr = (15×11)mm, the antenna's operational frequency shifted significantly,

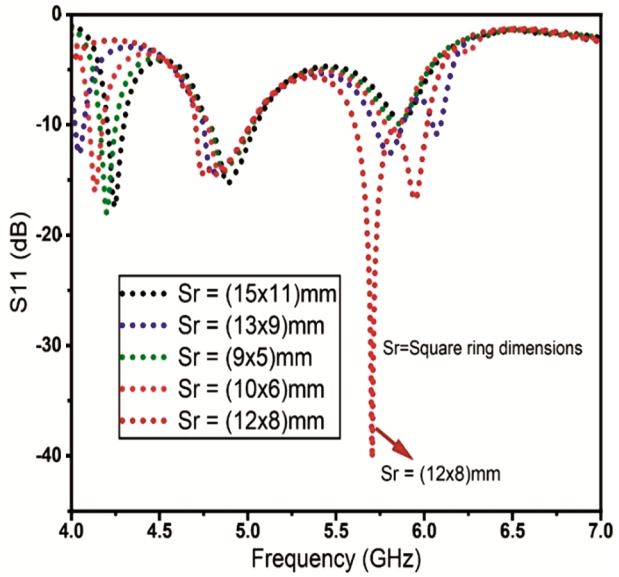


Fig. 13 — Parametric analysis of the central ring position (Sr)of the intended antenna.

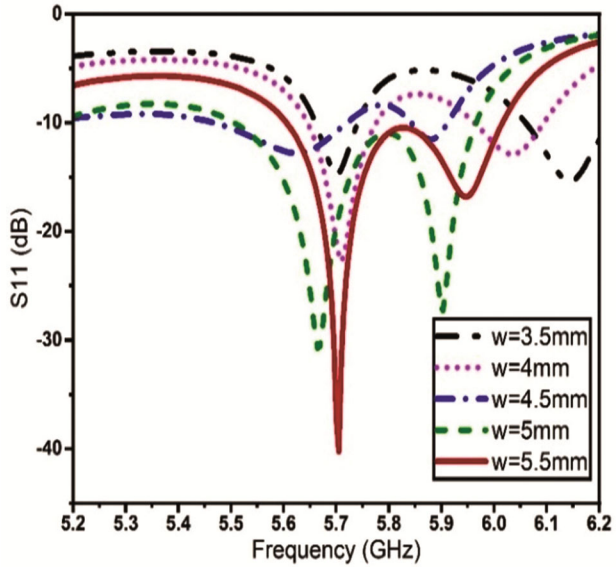


Fig. 14 — Parametric analysis of corner cut antenna reflection coefficients ($|S_{11}|$) for different slot width

manifesting itself at 4.25 GHz and 4.82 GHz. These values fell below the desired frequency range, indicating a crucial misalignment in the antenna's performance. After that, it is positioned at Sr =(13×9) mm and observed reflection coefficient ($|S_{11}|$) = -12.4 dB at 5.82 and resulting in narrow bandwidth. When the position of ring is set at value Sr = (9×5) mm and Sr = (10×6) mm, for both cases the antenna is not radiating in desired frequency range. Now the ring is positioned at (12×8) mm, a notable enhancement in the antenna's bandwidth, is indicated in WBAN frequency range. Furthermore, the QCCR antenna exhibits resonance at the frequency of 5.7 GHz with spanning bandwidth of 5.5GHz to 6 GHz. The next parameter under consideration for optimizing the intended antenna involves introducing a rectangular slot with dimensions of 8.5mm × 5.5 mm, which is cut at all the corners. To further enhance the antenna design, a parametric analysis is conducted on the slot width. The reflection coefficient analysis curve of the proposed antenna is illustrated in Fig. 14, showcasing the impact of variation slot width in x direction denoted by the parameter "$W_3$", ranging from 3.5mm to 5.5mm. Upon examination of the curve, it is observed that the reflection coefficient ($|S_{11}|$) reaches a value of -14.6dB when w is set to 3.5mm.

Notably, there is an improvement of -8dB when the position of the slot width in x direction is adjusted to $W_3$=4mm. Interestingly, for $W_3$= 4.5mm, antenna does not exhibit radiation in desired. However, at $W_3$=4mm, there is a merging of two frequency bands, resulting in an extension of the bandwidth. Surprisingly, opting for $W_3$= 5.5 mm yields dual benefits, both bandwidth extension and favourable reflection coefficients ($|S_{11}|$) in WBAN frequency range were achieved. curve shows the maximum signal transmission is achieved by the input impedance of antenna is matched with the 50Ω. The input resistance at feedline length ($W_4$) = 14.5 mm crossed the 50Ω line within the wireless BAN spectrum. Additionally, the separation distance (2mm) between the designed antenna and the human body is implemented to examine the radiation absorption by the human body (Fig. 3). The effects of separation distance between the antenna and human body to achieve low SAR value.

## 4 Results and Discussion

The proposed antenna is simulated in free space and with HUGO body phantom of VOXEL family and with the experimentally measured results. Here, the evolution of the implemented antenna patch structure is discussed (Fig. 1). The reflection coefficients, gain and radiation efficiency of each iteration is simulated and shown in Figs 5, 6 and 7, respectively. The radiation efficiency of all the iterations proposed antenna, the improvement in radiation efficiency is in iteration 4 observed. The designed antenna is simulated with body phantom to analyse the impact of SAR (Fig. 3). The SAR for the DGS technique-based antenna is 0.9W/Kg which is within the safety limits specified by the FCC.

The antenna's performance is further analysed by placing it on cylinder (to mimic the arm). After the bending analysis, it is observed that the antenna performance in both free space and on cylindrical surface analysis are showing the consistent results, depicted in Fig. 11. To optimize the antenna performance parametric analysis is performed on feedline width, corner slots and central ring the in free space. The reflection coefficient ($|S_{11}|$) of the feedline width, central ring and corner slot are shown in Figs. 12, 13 and 14, respectively. After the parametric analysis the feedline width is 2 mm, ring of 4 mm at Sr = (12×8) mm and corner slot dimensions (8.5×5.5) mm is considered. The fabricated antenna patch structure and DGS technique-based ground structure are shown in Fig. 15 (a-b), respectively. The experimental set up for measurement of fabricated antenna parameters are depicted in Fig. 16. The reflection coefficient ($|S_{11}|$) of proposed and fabricated antenna can be seen in Fig. 17. In all the three cases the antenna is resonating in desired WBAN frequency range. The resonating frequency of the proposed antenna is 5.69 GHz and 5.92 GHz, when simulated in free space, 5.77 GHz with body phantom and 5.78 GHz after fabrication. The reflection coefficient ($|S_{11}|$) of purposed antenna with body phantom is reduced as compare to the designed antenna without phantom due to loading effect of human body. The gain (dBi) of the designed antenna demonstrates the gain of 7.25 dBi in free space and 6.98 dBi with body phantom. This reduction in gain is due to loading effect of the body phantom and the surface current of antenna (Fig. 18). The experimentally measured antenna's gain is 1 dBi lower than the calculated gain with body phantom.

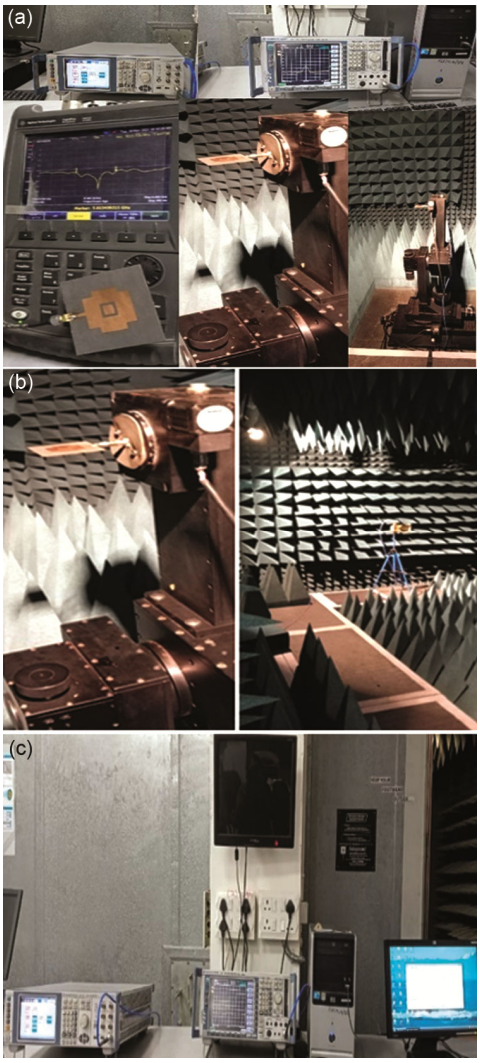


Fig. 16 — (a) Experimental setup of antenna parameter measurements, (b) $|S_{11}|$ measurement and radiation pattern measurement setup, and (c) Transmission and receiving antenna setup in ionic chamber

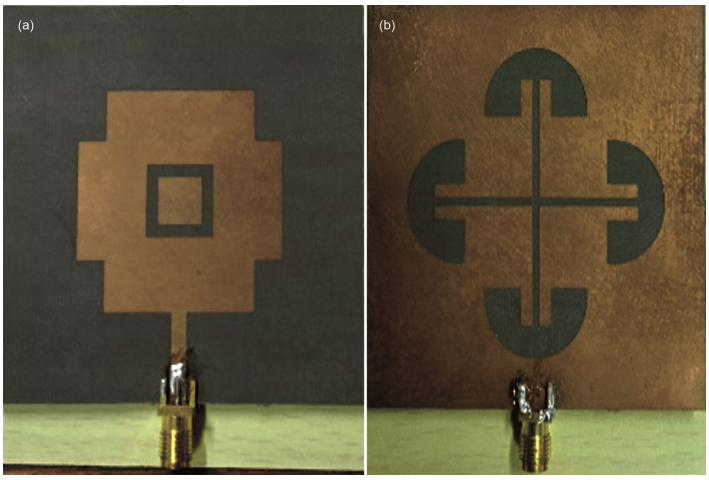


Fig. 15 — (a) Top view of the fabricated antenna, and (b) defective ground structure view of fabricated antenna

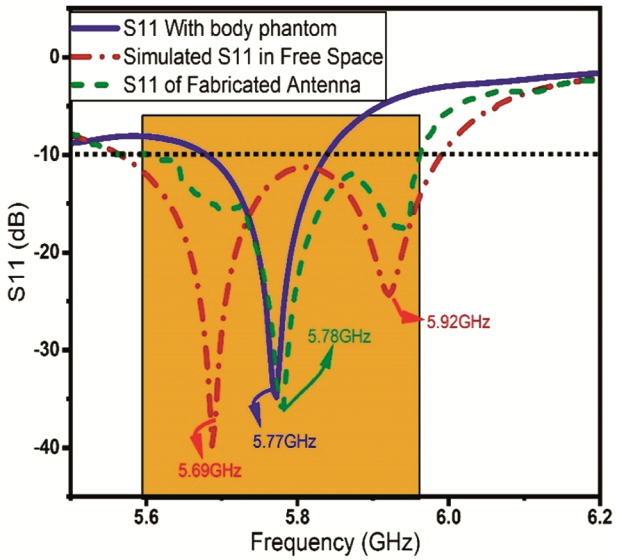


Fig. 17 — Reflection coefficient ($|S_{11}|$) of the Simulated antenna, fabricated and with body phantom of proposed antenna.

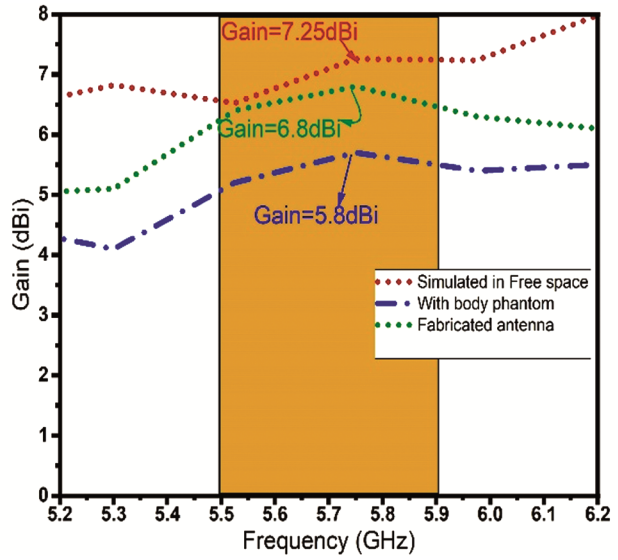


Fig. 18 — Gain (dBi) analysis of the simulated, fabricated and with body phantom of proposed antenna

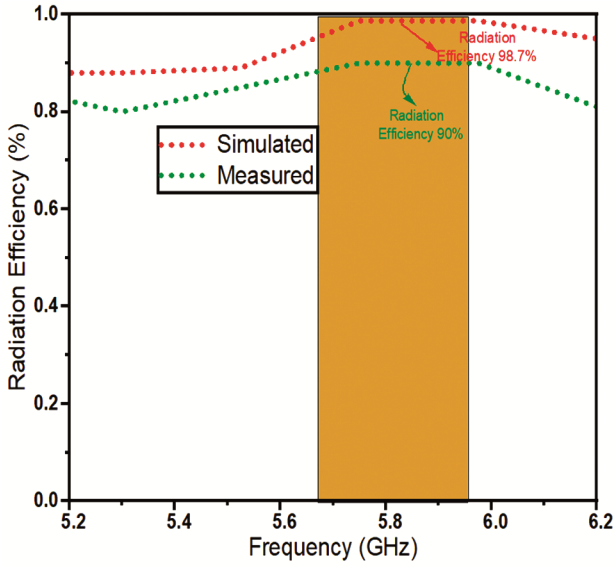


Fig. 19 — Simulated and measured radiation efficiency of proposed antenna

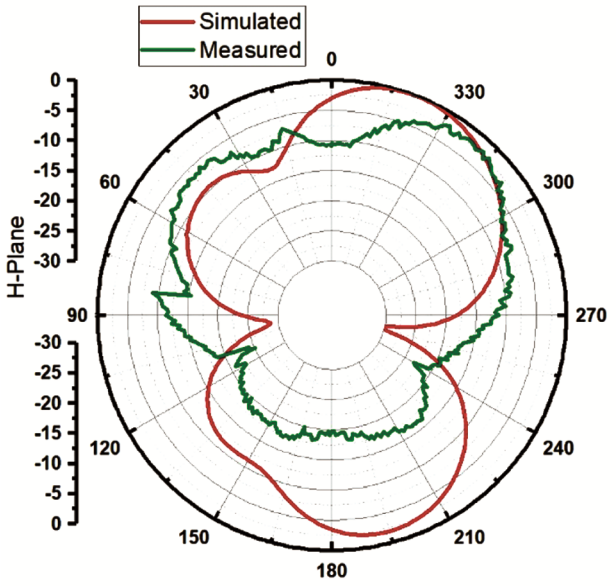


Fig. 20 — Simulated and measured H plane radiation pattern of proposed antenna

The simulated and fabricated antenna radiation efficiency of the antenna are 98.7% and 90% respectively (Fig. 19). The radiation pattern of the antenna was measured in an echo free anechoic chamber. Discrepancies between simulated and measured values are attributed cable losses and imperfections in measurement device calibration. The backward antenna radiation to the human body is reduced by placing the intended antenna 2mm above the body phantom (Fig. 5). Figure 20 represent the radiation pattern of H-plane of the proposed antenna in free space, with human body phantom and fabricated antenna. When the proposed antenna is affixed to the human body phantom, the back lobe is reduced. The simulated bandwidth is 500 MHz, while the measured bandwidth is 350 MHz. In Table 1 electrical properties of each layer of HUGO body phantom are discussed. Table 2 presents a comparative analysis, highlighting the advantages of the proposed antenna in the ISM band compared to existing biomedical antennas in terms of size, gain and SAR. Notably, the proposed antenna exhibits a

lower profile and higher fractional bandwidth, making it well-suited for biomedical applications. The proposed antenna demonstrates advantages in terms of its compact profile, wider fractional bandwidth, and suitability for biomedical applications. It has been observed that the antenna is insensitive to use in closed vicinity to the human body phantom. The optimization of antenna parameters has been done by using the CST software.

## 5 Conclusion

A low profile QCCR planar antenna for biomedical telemetry application has been simulated, fabricated and tested experimentally. The comparisons of intended antenna parameters SAR, bandwidth and gain with recent previous work were outlined in Table 2. This antenna resonates at 5.68GHz and 5.92GHz, exhibiting a -10dB bandwidth of 500 MHz A satisfactory agreement between the simulated and fabricated antenna parameter results has been observed. The proposed antenna exhibits with DGS showed the improvement in the bandwidth and gain. It is concluded from the simulated and experimentally measured results that the antenna robust behaviour against human body phantom loading and bending deformation. SAR is a crucial parameter for biomedical planar antennas, and its value should be below 1.6 W/Kg. The intended antenna attains a SAR value of 0.9 W/Kg, falling within the specified range outlined by FCC and IEEE guidelines.The simulated gain of the planar biomedical antenna is 7.25 dBi, while the measured gain is 6.98 dBi. The fabricated antenna exhibits outstanding performance and is well-suited for WBAN and biomedical telemetry applications.

## References


1 Yan A S, Soh P J &Vandenbosch G, *Electron Lett*, 50 (2014) 420.
2 Yan S & Vandenbosch G A E, *IEEE AntennasWireless Propag Lett*, 15 (2016) 1715.
3 Alemaryeen A & Noghanian S, *Proc United States Nat Committee URSI Nat Radio Sci Meetings*, 2017, 1.
4 Hossain A, Wagner S, Pancrazio S & Pham A V*, IEEE International Symposium (APS/URSI),* 2021, 51.
5 Kumari L, Khan M, Sani M M, Zahreeuddin & Khan M A, *International Conference on Recent Advances in Electrical, Electronics & Digital Healthcare Technologies(REEDCON*), New Delhi, India, 2023, 236.
6 Gao G, Hu N, Wang S & Yang C, *, Microwave Opt Technol Lett*, 60 (2018) 876.
7 Balanis A, *Antenna Theory: Analysis and Design*, (United States: John Wiley & Sons), 3rd Edition, 2015.
8 Guan C E & Fujimoto T, *Electron*, 9, 2020.
9 Khan M, Kumari L, Sani M M, Zahreeuddin & Salhan A, *Energ Contr (PIECON*), 2023.
10 Yan A S, Soh P J & Vandenbosch G, *Electron Lett*, 50 (6) (2014) 420.
11 Arif A, Zubair M, Ali M, Khan M U & Mehmood M Q, *IEEE Antennas Wireless Propag Lett*, 18 (2019) 981.
12 Mohan C & Florence S E*, , IETE J Res*, 2019, 1.
13 Li Y J, LuZ Y & Yang L S*, IEEE Access,* 7 (2019) 42107.
14 Zhu S & Langley R, *IEEE Trans Antennas Propag,* 57 (4) (2009) 926.
15 Zhu X Q, Guo Y X &Wu W, *IEEE Antennas Wireless Propag Lett,* 15 (2016) 98.
16 Klemm, Locher I & Troster G, *Eur Conf Wireless Technol,* 2004, 285
17 Jan J Y & Su J W, *IEEE Transactions on Antennas and Propagation,* 53 (6) (2005) 2111.
18 Sung Y, *IEEE Transactions on Antennas and Propagation*, 60 (4) (2012) 1712.
19 Chiang K H &Tam K W,*IEEE Antennas Wireless Propag Lett,* 7 (2008) 532.
20 Kumar C & Guha D, *IET Microwave*, 8(2014) 589.
21 Zubair A M, Ali M, Khan M U & Mehmood M Q, *IEEE Antennas Wireless Propag Lett,* 18 (5) (2019) 981.
22 Smida A, Iqbal A, Alazemi A J, Waly M I, Ghayoula R & Kim S, *IEEE Access,* 8 (2020) 15687.
23 Khan M, Kumari L & Zaheeruddin Z, *Ind J Pure Appl Phys,* 62 (2024) 884.
24 El Atrash M, Abdalla M A & Elhennawy H M, *IEEE Trans Antennas Propag,* 67 (10) (2019) 6378.
25 Mantash M, Tarot A C, Collardey S & Mahdjoubi K, *Electron Lett*, 5 (2016) 95.
26 Yan S, Soh P J &Vandenbosch G A E, *IEEE Trans Antennas Propag,* 62 (12) ( 2014) 6487.
27 Zhu S & Langley R, *IEEE Trans Antennas Propag,* 57 (2009) 926.
28 Abbasi M A B, Nikolaou S S, Antoniades M A, Stevanovi M N & Vryonides P, *IEEE Trans Antennas Propag,* 65 (2017) 453.
29 Alemaryeen A & Noghanian S, *IEEE Transactions on Antennas and Propagation*, 67 (6) (2019) 3649.
30 Yin B, Ye M & Yu Y, *Progress In Electromag Res C*, 107 (2021) 97.
31 AshyapA Y I, *IEEE Access*, 6 (2018) 77529.